AIAA 80-0033R

Simplified Solution of the Compressible Lifting Surface Problem

James W. Purvis*
Sandia National Laboratories, Albuquerque, N. Mex.
and
John E. Burkhalter†
Auburn University, Ala.

A simplified application of planar lifting-surface theory is presented for determining the load distribution on finite wings in compressible subsonic flow. Classical theoretical forms are used to define functions for the pressure coefficient distribution. The Kernel function integral is evaluated in a closed form/finite summation manner, resulting in a well-behaved coefficient matrix similar to that obtained in vortex lattice theory. The Mangler-type singularity is avoided. Chordwise and spanwise integrals for lift and induced drag are reduced to simple summation, with the number of terms equal to the number of collocation points used. Analytical results are compared with experimental data and with other methods; quick convergence and computational efficiency are illustrated.

Nomenclature

$\mathcal{R}$	= aspect ratio
b	= wingspan
c	= local wing chord
$\bar{c}$	= mean aerodynamic chord; reference length
cc_d	= section drag force/q_∞
cc_l	= section lift force/q_∞
c^2c_m	= section pitching moment/q_∞
C_{D_i}	= induced drag coefficient
C_L	= lift coefficient
C_m	= pitching moment coefficient
C_p	= pressure coefficient $(p-p_\infty)/q_\infty$
ΔC_p	= pressure loading coefficient; difference between upper- and lower-surface pressure coefficients at a point
$K(x_1,y_2)$	= partial influence function [see Eq. (10)]
M_∞	= freestream Mach number
S	= wing planform area; reference area
V_∞	= freestream velocity
V	= velocity vector
w	= nondimensional perturbation velocity W/V_∞; parallel to z axis
x,y,z	= Cartesian coordinates; origin at wing apex, $+x$ streamwise, $+y$ along right wing panel as viewed looking upstream
x_{LE}	= distance from y axis to leading edge of wing
x_0,y_0	= dummy variables
α	= angle of attack
β	= Mach parameter, $\sqrt{1-M_\infty^2}$
γ	= nondimensional vorticity; Γ/V_∞
Λ	= wing sweep angle
λ	= taper ratio; tip chord/root chord
ϕ	= nondimensional perturbation velocity potential; Φ/V_∞
ξ	= nondimensional chordwise variable; $(x-x_{LE})/c$
η	= nondimensional spanwise variable; $y/(b/2)$
θ	= spanwise angular variable defined by $\theta=\cos^{-1}(\eta)$

Subscript

∞	= freestream conditions

Introduction

SINCE the advent of Prandtl's hypothesis, potential-flow methods have been used increasingly in the design and analysis of aerodynamic configurations (e.g., Refs. 1-3). For most aerodynamic configurations, the wing is still the primary load-carrying surface; thus the foundation of an analytical method must be an adequate lifting-surface analysis. The continued interest in developing adequate wing analyses was perhaps best illustrated at a recent NASA conference,[4] where increased accuracy, reduced computational time, generality, and flexibility were emphasized.

Current lifting-surface methods are loosely divided into two groups: discrete elements (such as vortex or doublet lattice) and distributed singularity (Kernel function or functional expansion) methods. Vortex lattice theory and application are well covered in Ref. 4, and excellent summaries are discussed in Refs. 5 and 6. At present, discrete-element methods appear to be the favored approach.

The Kernel function method, however, is still widely used,[7-12] with a summary and discussion of capabilities presented in Ref. 13. This method is particularly useful where time-dependent loadings are involved[14] and inherently would appear to be a better overall model of the physical flow.

The appeal of the Kernel function approach, as opposed to a discrete-element method, such as vortex lattice, is due to several reasons. The solution provides a continuous and realistic ΔC_p distribution, and the flow tangency condition may be very nearly satisfied over the entire wing. As compared with discrete-element methods, using the Kernel function approach, relatively few unknowns are required for an adequate, converged solution. The accuracy of the Kernel function solution, however, is dependent on both the functional form chosen for ΔC_p and the manner and accuracy with which the surface integral is evaluated, particularly near the control point singularities. Several ingenious schemes for dealing with evaluation of the discontinuity in the Kernel and numerical integration across the second-order singularity at each control point are available (e.g., Ref. 15), but these generally involve complicated mathematics and, hence, complex computer codes. As with the vortex lattice method, the number and placement of control points (points where the tangency condition is satisfied) have a significant effect on the solution.

Presented as Paper 80-0033 at the AIAA 18th Aerospace Sciences Meeting, Pasadena, Calif., Jan. 14-16, 1980; submitted Feb. 7, 1980; revision received Sept. 14, 1981.

*Member of the Technical Staff, Aerodynamics Department. Member AIAA.

†Associate Professor, Aerospace Engineering Department. Member AIAA.

A somewhat different approach is presented by Lan[16] wherein the downwash equation contains Cauchy-type integrals as opposed to Mangler-type integrals in the Kernel function formulation. DeJarnette[17] extended the strip approach of Lan to provide for "continuous" loading in the spanwise direction. Results of the Lan-DeJarnette formulation offer an improvement over the vortex lattice approach but unfortunately contain a midspan singularity that is not well understood.

The objective of the present investigation is to present a method for using the distributed singularity approach that will retain the advantages of the theory while eliminating some of the inherent problems. In this connection, lifting line, thin airfoil, and slender wing theory results are used to develop a general functional form for the ΔC_p distribution, and the basic integral equation is expressed in terms of vorticity that satisfies the linearized compressible potential equation. Additionally, improvements in the theory are included which more accurately account for taper ratio and planform shape.

Evaluation of the integral is done in a closed form/finite summation manner that eliminates the need for numerical integration and the requisite use of a principal-value method, such as the Mangler technique, near control points. This evaluation leads to a well-conditioned coefficient matrix since the integral results are remarkably similar to the vortex lattice equations. Use of the Multhopp spacing for control points, in conjunction with the above, produces accurate flow tangency over the entire wing without the use of a least-squares formulation. Simple finite-sum expressions result for section and total forces and moments, similar to those obtained from thin airfoil and lifting line analyses. In comparison with other discrete-element and lifting-surface methods, the present approach is shown to reduce computation time considerably (in some cases, by an order of magnitude), and computer storage requirements are minimal.

Analysis

The derivation of the well-known incompressible lifting-surface integral equation is available in any good reference on theoretical aerodynamics. The usual correction for Mach number employed in analysis of planar wings is the Prandtl-Glauert-Goethert similarity rule. This procedure is not necessary provided the Kernel in the lifting-surface integral satisfies the linearized compressible potential equation. With this condition in mind, the potential equation for a planar lifting surface in compressible subsonic flow may be shown to be

$$\phi(x,y,z) = \frac{1}{4\pi}\iint_S \frac{\gamma(x_0,y_0)}{(y-y_0)^2+z^2} z \times \left[1+\frac{x-x_0}{\sqrt{(x-x_0)^2+\beta^2(y-y_0)^2+\beta^2 z^2}}\right] dx_0 dy_0 \qquad (1)$$

which differs from the incompressible results only by the β^2 terms in the radical.

Using the relation between the surface vorticity strength and the pressure loading coefficient, $\gamma = \Delta C_p/2$, the nondimensional normalwash in the plane of the sheet due to the sheet itself is

$$w(x,y) = \frac{1}{8\pi}\iint_S \frac{\Delta C_p(x_0,y_0)}{(y-y_0)^2} \times \left[1+\frac{x-x_0}{\sqrt{(x-x_0)^2+\beta^2(y-y_0)^2}}\right] dx_0 dy_0 \qquad (2)$$

Introducing dimensionless spanwise and chordwise variables η and ξ, the ΔC_p expression can be written as a combination of spanwise and chordwise terms in which the behavior along a chord line or across the span can be examined independently. Since the loading along each chord line should behave in the classical two-dimensional manner at the leading and trailing edges, thin airfoil theory results can be used to define ΔC_p as

$$\Delta C_p(\xi,\eta) = \sqrt{\frac{1-\xi}{\xi}} \sum_{n=0}^{N} H_n(\eta) G_n(\xi) \qquad (3)$$

In thin airfoil theory, the G_n functions are Fourier terms. The Fourier terms could easily be used in the present analysis; however, for convenience in later equations, these functions are defined as simple polynomial terms:

$$G_n(\xi) = \xi^n \qquad (4)$$

Although this form for the chordwise loading is a nonorthogonal set, it should be noted that the weighting function $\sqrt{(1-\xi)/\xi}$ forces each chordwise term to satisfy the Kutta condition, and the first term in Eq. (3) has the required leading-edge singularity. In addition, the product of G_1 with the weighting function produces the classical parabolic camber loading results where the vorticity is proportional to $\sqrt{\xi(1-\xi)}$. Higher-order terms produce other camber shapes, and this particular form for G_n yields a convenient recursion relation when integrated.

Lifting line theory indicates that the spanwise functions $H_n(\eta)$ should be elliptic in nature for finite values of taper ratio, and for zero taper ratio, the required behavior is that of slender wing theory. Introducing the spanwise angular variable θ, a functional form satisfying both these requirements is

$$H_n(\eta) = \frac{1}{c(\eta)} \sum_{m=0}^{M} B_{nm} \sin(2m+1)\theta \qquad (5)$$

where

$$\theta = \cos^{-1}(\eta) \qquad (6)$$

The B_{nm}'s are constant coefficients, and $c(\eta)$ is the local chord. On a trapezoidal wing with zero taper ratio and a unit root chord, the $m=0$ term reduces to $\sqrt{1+\eta}/\sqrt{1-\eta}$, which has the required slender wing behavior near the wing tips. For a taper ratio of 1.0, the classical elliptic loading term $\sqrt{1-\eta^2}$ is obtained from the $m=0$ term. Combining Eqs. (3-5), the complete expression for the pressure loading coefficient becomes

$$\Delta C_p(\xi,\eta) = \sum_{n=0}^{N} \frac{1}{c(\eta)} \sum_{m=0}^{M} B_{nm} \sin(2m+1)\theta \sqrt{\frac{1-\xi}{\xi}}\, \xi^n \qquad (7)$$

Returning to the evaluation of the downwash, note that, over a sufficiently small element of the planform surface, ΔC_p is approximately constant and so can be taken outside the integral. This procedure is analogous to the constant-panel-loading assumption that is fundamental to the discrete-element theories. The downwash due to this small element then becomes

$$\Delta w(x,y) = \frac{\Delta C_p(\bar{x},\bar{y})}{8\pi} \int_{y_1}^{y_2}\int_{x_1}^{x_2} \frac{1}{(y-y_0)^2} \times \left[1+\frac{x-x_0}{\sqrt{(x-x_0)^2+\beta^2(y-y_0)^2}}\right] dx_0 dy_0 \qquad (8)$$

where $\Delta C_p(\bar{x},\bar{y})$ is evaluated at the centroid of the element. The integral thus obtained can be evaluated in closed form with the results

$$\Delta w(x,y) = \frac{\Delta C_p(\bar{x},\bar{y})}{8\pi}\left[K(x_2,y_2) - K(x_2,y_1) - K(x_1,y_2) + K(x_1,y_1)\right] \tag{9}$$

where, for example

$$K(x_1,y_2) = -\frac{(x-x_1)+\sqrt{(x-x_1)^2+\beta^2(y-y_2)^2}}{y-y_2} + \beta\log_e\left[\beta(y-y_2)+\sqrt{(x-x_1)^2+\beta^2(y-y_2)^2}\right] \tag{10}$$

The other K's of Eq. (9) are evaluated by making the appropriate substitution of the subscripted variables in Eq. (10).

If the entire planform is divided into similar small elements, the total downwash at any point on the wing surface may be written as

$$w(x,y) = \sum_S \Delta w(x,y) \tag{11}$$

where Eqs. (7), (9), and (10) are used to evaluate each Δw.

The nondimensional tangency condition for small angles of attack is

$$w(x,y) + \alpha(x,y) = 0 \tag{12}$$

which defines the load distribution in terms of the physical requirement of no flow through the wing. The chordwise and spanwise control points are determined from cosine distributions[17] as

$$x_i = x_{\mathrm{LE}}(y_j) + \frac{c(y_j)}{2}\left(1-\cos\frac{\pi i}{N+1}\right), \quad i=1,2,\ldots,N+1$$

and

$$y_j = \frac{b}{2}0.5\left(1-\cos\frac{\pi j}{M+1}\right), \quad j=1,2,\ldots,M+1 \tag{13}$$

In order to avoid singularity problems, the control point locations are adjusted slightly to coincide with the centroid of the subelement on which they lie. Equation (12) is then evaluated at each control point, resulting in

$$\sum_S \Delta w(x_i,y_j) + \alpha(x_i,y_j) = 0 \tag{14}$$

Equation (14) together with the defining relations (7) and (9) constitute a set of simultaneous linear algebraic equations for $(N+1)\times(M+1)$ unknown loading coefficients B_{nm}. Solving the system for these coefficients, the pressure loading at any point on the wing is then available from Eq. (7).

The spanwise section loading is given by

$$cc_l(\eta_0) = c(\eta_0)\int_0^1 \Delta C_p(\xi,\eta_0)\,\mathrm{d}\xi \tag{15}$$

This integration can be done in closed form. Defining

$$I_n = \int_0^1 \xi^n\sqrt{\frac{1-\xi}{\xi}}\,\mathrm{d}\xi, \quad n=0,1,\ldots,N \tag{16}$$

and integrating yields

$$I_0 = \pi/2$$

and the recursion relation

$$I_n = \frac{2n-1}{2n+1}I_{n-1}, \quad n=1,2,\ldots,N \tag{17}$$

For convenience, let

$$E_m = \sum_{n=0}^{N} B_{nm}I_n \tag{18}$$

Then after substitution into Eq. (15) from Eqs. (7), (16), and (18) successively,

$$cc_l(\eta_0) = \sum_{m=0}^{M} E_m \sin(2m+1)\theta_0 \tag{19}$$

Similar manipulations lead to

$$c^2 c_{m_{\mathrm{LE}}}(\eta_0) = -c(\eta_0)\sum_{m=0}^{M}\sum_{n=0}^{N} B_{nm}I_{n+1}\sin(2m+1)\theta_0 \tag{20}$$

and in the far field to

$$cc_d(\eta_0) = \frac{cc_l(\eta_0)}{8}\sum_{m=0}^{M}(2m+1)E_m\frac{\sin(2m+1)\theta_0}{\sin\theta_0} \tag{21}$$

for the pitching moment about the local leading edge and section drag, respectively. The total lift and induced drag are found by evaluating the standard integral forms

$$C_L = \frac{1}{S}\int_{-b/2}^{b/2} cc_l(\eta_0)\,\mathrm{d}\eta_0 \tag{22}$$

and

$$C_{D_i} = \frac{1}{S}\int_{-b/2}^{b/2} cc_d(\eta_0)\,\mathrm{d}\eta_0 \tag{23}$$

Using the spanwise angular variable θ and Eqs. (19) and (20) in the above gives

$$C_L = \pi E_0/2S \tag{24}$$

and

$$C_{D_i} = \frac{\pi}{16S}\sum_{m=0}^{M}(2m+1)E_m^2 \tag{25}$$

These resemble the classical forms obtained from Glauert's lifting line analysis.

The total pitching moment about the wing apex (y axis) is given by

$$C_m = \frac{1}{S\bar{c}}\int_{-b/2}^{b/2}\left[c^2 c_m(\eta_0) - x_{\mathrm{LE}}(\eta_0)cc_l(\eta_0)\right]\mathrm{d}\eta_0 \tag{26}$$

The integral in Eq. (26) cannot be evaluated in closed form unless simple functional expressions for $x_{\mathrm{LE}}(\eta_0)$ and the local chord term in $c^2c_m(\eta_0)$ are known. For the case of a simple

trapezoidal planform

$$x_{LE}(\eta_0) = \eta_0 \tan\Lambda \tag{27}$$

and

$$c(\eta_0) = c_R - [(c_R - c_T)\eta_0] \tag{28}$$

Using these equations, the pitching moment is

$$C_m = \frac{1}{Sc}\left[(c_R - c_T)\sum_{m=0}^{M} F_m J_m - \tan\Lambda \sum_{m=0}^{M} E_m J_m - \frac{\pi}{2} c_R F_1\right] \tag{29}$$

where

$$F_m = \sum_{n=0}^{N} B_{nm} I_{n+1} \tag{30}$$

and

$$J_m = \int_0^{\pi/2} \sin 2\theta_0 \sin(2m+1)\theta_0 \, d\theta_0 = -\frac{2\cos m\pi}{(2m+3)(2m-1)} \tag{31}$$

For sharp-edged wings, the method of Ref. 18 may be used to predict the additional lift and moment due to separated flow about the wing leading edge. For example, the leading-edge vortex lift for a wing with constant sweep angle is

$$C_{L_{VLE}} = (C_L \sin\alpha - C_{D_i}\cos\alpha)(\cos\alpha/\cos\Lambda) \tag{32}$$

where C_L and C_{D_i} are given by Eqs. (22) and (23), respectively.

Expressions are also developed in Ref. 18 for determining leading-edge and side-edge vortex lift and moment distributions on wings with sweep angles that are functions of span.

Results and Conclusions

Flow Tangency

The present theoretical results were compared extensively with experimental data to determine the accuracy of flowfield modeling. One method of determining accuracy is determining how well the lifting surface is modeled as a solid body. For the more difficult case of a delta wing, less than 2% deviation (0.02α) from the desired zero net normalwash is obtained over most of the wing surface. The only significant deviation is near the leading edge, where deviations on the order of 10% were obtained; even this error is considered minor when compared with a vortex lattice formulation.

Control Point Placement, Polynomial Order, and Element Size

For the present theoretical results, the best control point distribution scheme was found to be Eq. (13), which in effect gives maximum surface coverage, as verified by DeJarnette.[17] In addition to the control point distribution, the effects of polynomial order, Eq. (7), and subelement size were also investigated.

The order of these polynomials defines the number of unknown coefficients to be determined and hence the size of the matrix to be inverted. In most cases it was found that three collocation points along the chord (second degree polynomial in ξ) and four points along the span (third order in η) produced acceptable results. Slightly better accuracy is obtained in going from the (3×4) twelve control points to (4×5) twenty points but usually does not warrant the increased central processing unit (CPU) time. Higher-order corrections up to 60 to 70 terms were also investigated, with acceptable results.

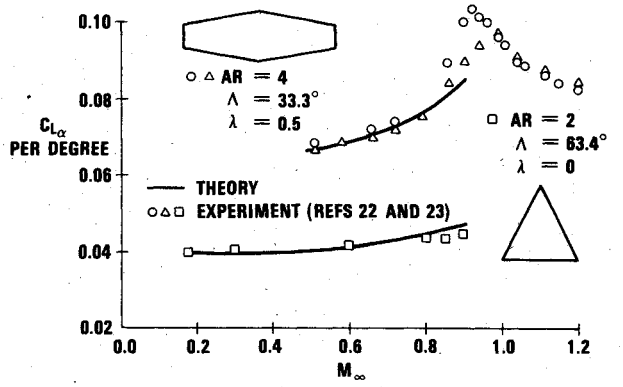

Fig. 1 Mach number effect on lift curve slope for two thin wings.

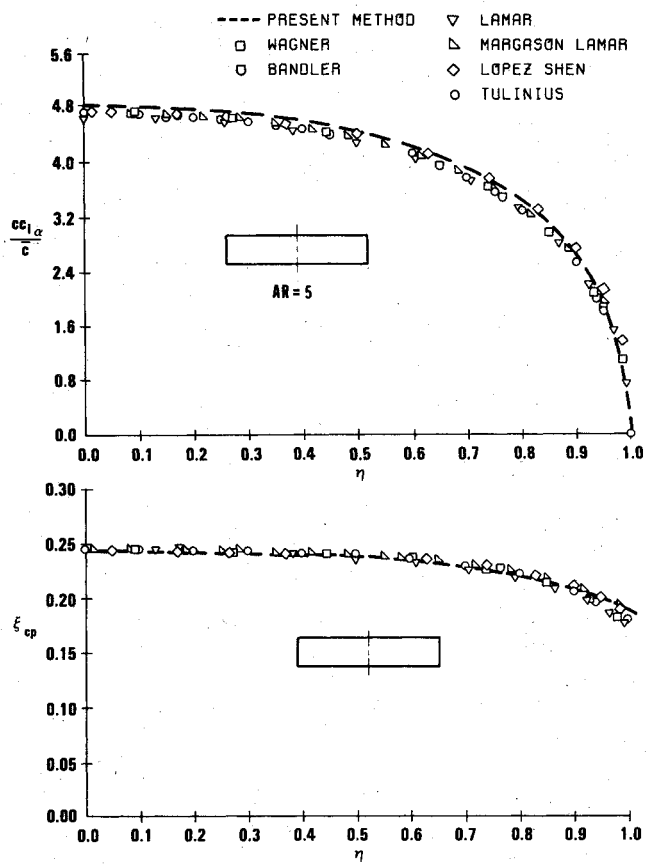

Fig. 2 Sectional lift and center-of-pressure variation for a rectangular wing of aspect ratio 5.

Similar effects were noted regarding the size of the integration element over which ΔC_p is assumed constant. Adequate results were obtained using sizes of 1/45th the local chord and semispan. Accuracy is enhanced by using smaller elements near leading edges, trailing edges, and wing tips. Note that these large numbers of elements appear only under the summation equation and consequently do not determine the order of the coefficient matrix, as in vortex lattice procedures.

Compressibility

Compressibility terms are included in the potential equation in a linearized form, and thus the theory should apply throughout the "linear" range. Comparison of the present theory with experimental results for low-$\mathcal{A}$ delta wing and a moderate-$\mathcal{A}$ tapered wing is shown in Fig. 1, where the effects of Mach number at subsonic speeds on the lift curve

slope are illustrated. Although only twelve collocation points (3×4 mesh) were used, the resulting agreement between theory and experiment is excellent for Mach numbers less than approximately 0.85. The agreement above $M=0.6$ is due to two factors: 1) both wings are ideally suited to a planar wing analysis since the thickness-to-chord ratio of each wing section is less than 5%, and 2) the experimental C_{L_α}'s were evaluated at low angles of attack.

Load Distribution

In further comparison with experiment and with other methods, the results of Ref. 19, which compared and evaluated 6 different applications of lifting-surface theory, were used extensively. These methods were selected, based on their agreement with each other and experiment, from among 15 methods evaluated in a previous study.[20]

To illustrate the nominal agreement between the various theories, span loading and chordwise center-of-pressure distributions for an unswept, untapered wing of $\mathcal{R}=5$ are compared in Fig. 2. Variations in span loading are about 2% among all the methods. The slightly higher section lift values of the current method are evidently due to the method of integration of the chordwise term $\sqrt{(1-\xi)/\xi}$, which determines the area near the singularity exactly. This supposition is lent credence by the fact that ξ_{CP} is slightly forward of the other values over most of the span.

Figures 3-8 present comparisons of theoretical and experimental results for three wings of various $\mathcal{R}$ and taper ratio. Calculated variables include span load distribution, spanwise centers of pressure, and chordwise distribution of ΔC_p at specified spanwise stations. The present method exhibits the same tendencies as the other theories, i.e., overprediction of ΔC_p near the leading and trailing edges and underprediction in the midchord region. Differences near the leading edges result from the finite thickness of the experimental models, and overprediction near the trailing edges is due to thickness and boundary-layer effects. Errors in both regions can be significantly reduced if thickness is taken into account, as will be shown subsequently. For the thinner wings, the span loadings verify the potential-flow prediction that thickness has a second-order effect on lift.

Comparison of the present theory was also made with Lan's quasi-vortex lattice method,[16] and results for one swept configuration are presented in Fig. 9. Agreement between the two theories is quite close; however, 41 spanwise collocation points are required for the Lan method and 4 points were used for the present approach.

In further comparison with Lan's method, from Fig. 1, the present method gives a C_{L_α} of 2.29/rad for the $\mathcal{R}=2$ delta wing, which is almost exactly the experimental result. By comparison, Lan's value for the same wing is 2.4707 from his Table 4.

Pitching Moment and Induced Drag

The calculation of pitching moment and far field induced drag also provides a measure of how well the pressure and load distributions are predicted. Of particular interest, in light of current design trends, is the capability of a method to accurately predict the forces and moments of planforms with variable leading-edge sweep. Values for total lift, drag, and pitching moment for two cranked wings and an ogee wing are shown in Figs. 10-12. The present method was used to compute the linear terms in the usual manner. The nonlinear terms are computed from the present theory according to the

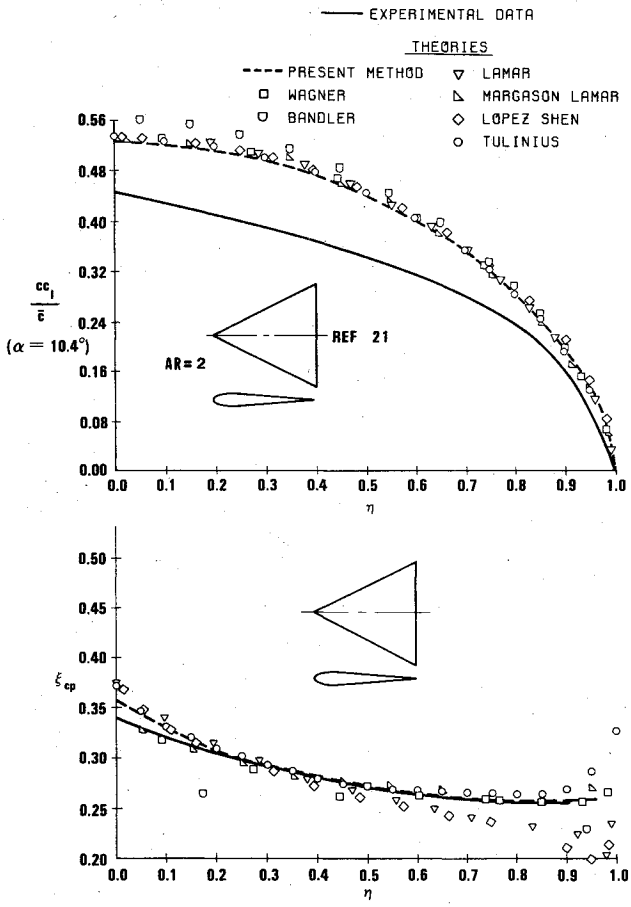

Fig. 3 Sectional lift and center-of-pressure variation for a delta wing; $\mathcal{R}=2$, $\alpha=10.4$ deg.

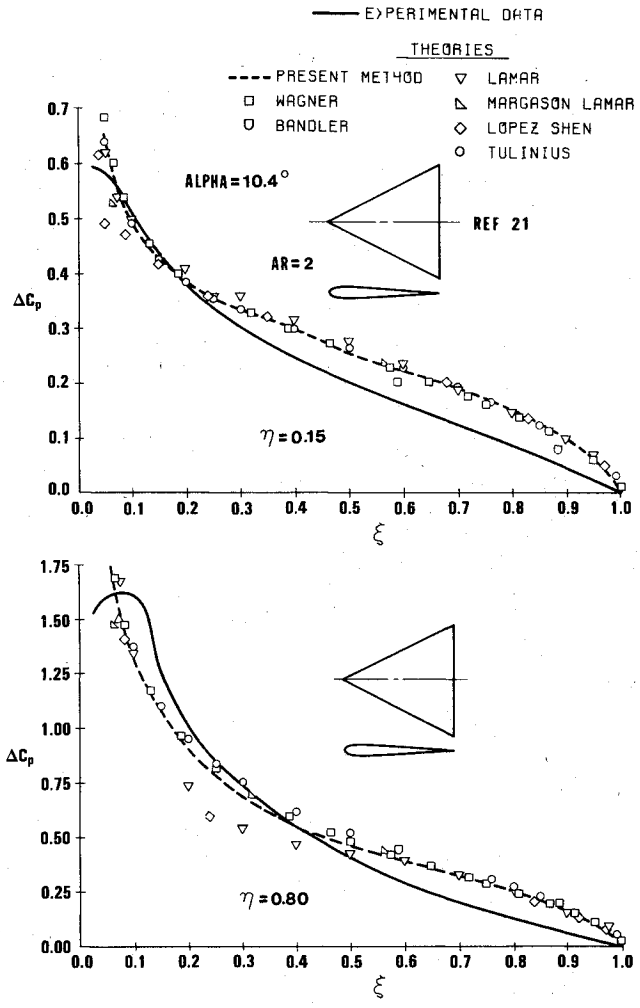

Fig. 4 Chordwise pressure variation for a delta wing; $\mathcal{R}=2$, $\alpha=10.4$ deg, $\eta=0.15$ and 0.80.

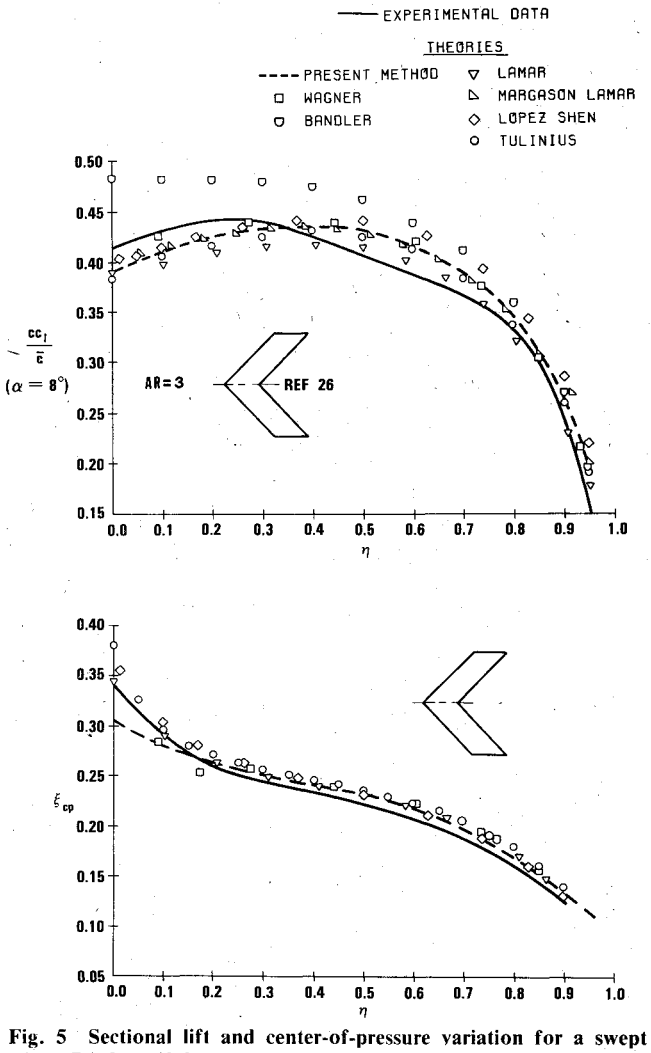

Fig. 5 Sectional lift and center-of-pressure variation for a swept wing; $\mathcal{R}=3$, $\alpha=8$ deg.

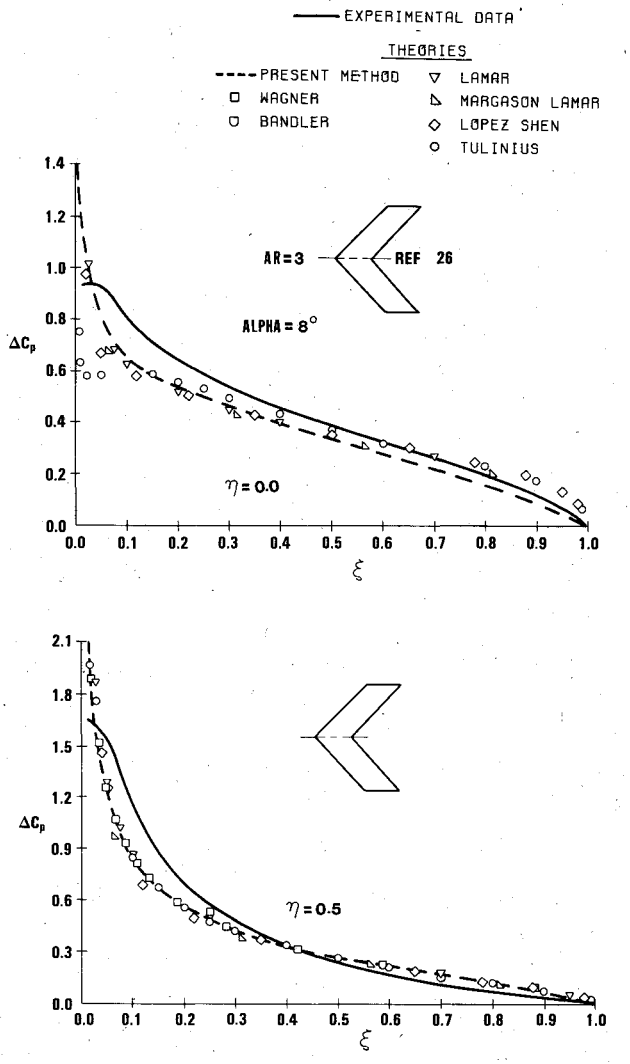

Fig. 6 Chordwise pressure variation for a swept wing; $\mathcal{R}=3$, $\alpha=8$ deg, $\eta=0.0$ and 0.5.

method of Ref. 18, which is based on the Polhamus suction analogy. The results compare extremely well with experiment, well into the nonlinear angle-of-attack range.

Thickness

In the light of the excellent agreement for C_{L_α} of the thin delta wing in Fig. 1, a possible cause of the errors in comparison with the thick delta wing case (Fig. 3) was investigated. Since the lift curve slope for the experiment[21] is nearly linear up to the stall, the errors are obviously not due to formation of a leading-edge separation vortex characteristic of sharp-edged, low $\mathcal{R}$ wings. It was postulated that the cause was a combination of thickness, aspect ratio, and taper ratio, giving rise to significant spanwise surface slopes, particularly near the leading edge.

Using two-dimensional thickness approximations and satisfying the tangency condition on the wing surface as opposed to the mean camber surface produced the results in Figs. 13 and 14. It is evident from these curves that errors between the thin wing theory results and experiment (Fig. 4) are primarily due to the fact that ΔC_p near the leading edge tends to zero in the physical case whereas theoretically it is infinite. The predicted lift coefficient based on the results in Fig. 13 was between the two given by experimental pressure integration and experimental force measurements.

Computer Execution Times

As repeatedly stressed in Ref. 4, computational efficiency is a major factor in the utilization of current theories. The range of execution times required for a single planform case is shown in Table 1, which is adopted from Ref. 19. These times refer to running times on a CDC 6700 system and are given in terms of 6400 CPU times; compile times are not included. The Lopez-Shen values are estimated based on the relative speeds of 6400 and the IBM 370/165.

Table 1 Range of execution times for single planform case

Program	Execution time (s)
Margason-Lamar[24]	110-120
Lopez-Shen[25]	170-210
Tulinius[9]	60-65
Bandler[10]	6-9
Lamar[11]	$\simeq 122$[a]
Wagner[12]	90-120
Lan[16]	$\simeq 17$-30[b]
Present method	$\simeq 14$

[a] Based on 4 chordwise and 15 spanwise control points, Ref. 11 states that at least this number are required for convergence of section load distributions. [b] Based on estimates of Lan's comparison with the Wagner program.

With the exception of Lan's program and the Bandler program, the current method is 3 to 10 times as fast as the other techniques. The speed advantage of the Bandler method, however, is more than offset by its consistently poor agreement with experiment. The time given for the present

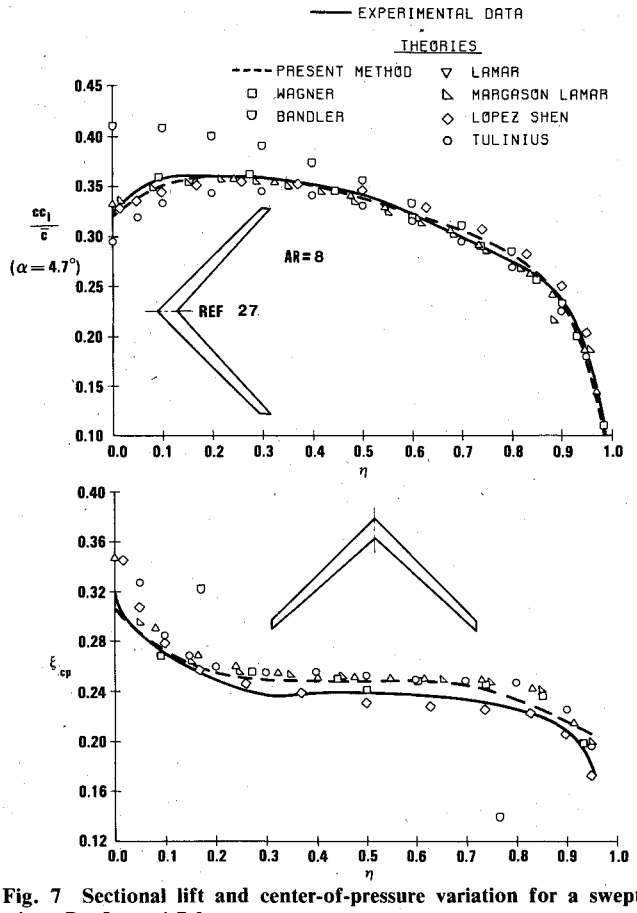

Fig. 7 Sectional lift and center-of-pressure variation for a swept wing; $\mathcal{R}=8$, $\alpha=4.7$ deg.

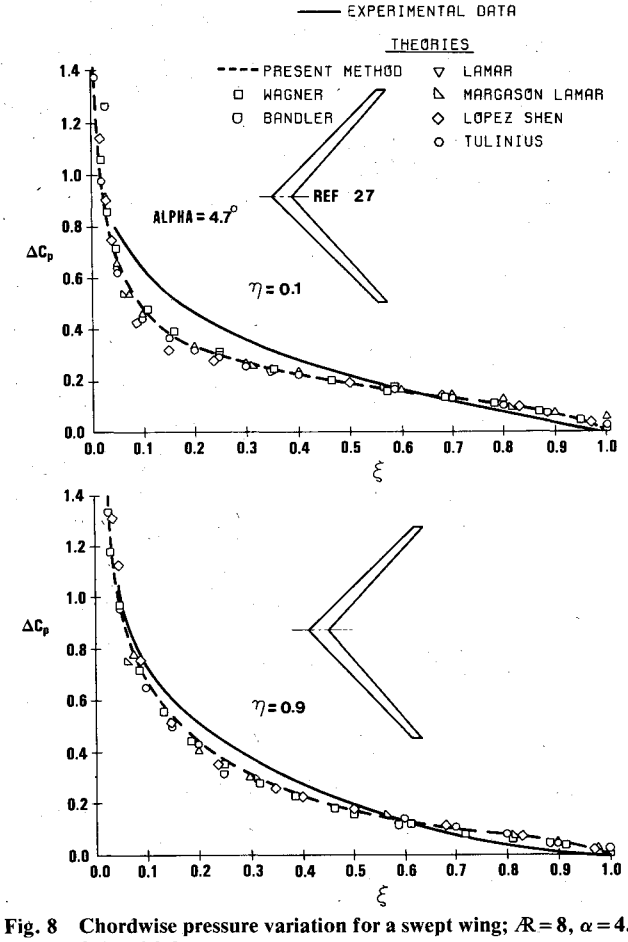

Fig. 8 Chordwise pressure variation for a swept wing; $\mathcal{R}=8$, $\alpha=4.7$ deg, $\eta=0.1$ and 0.9.

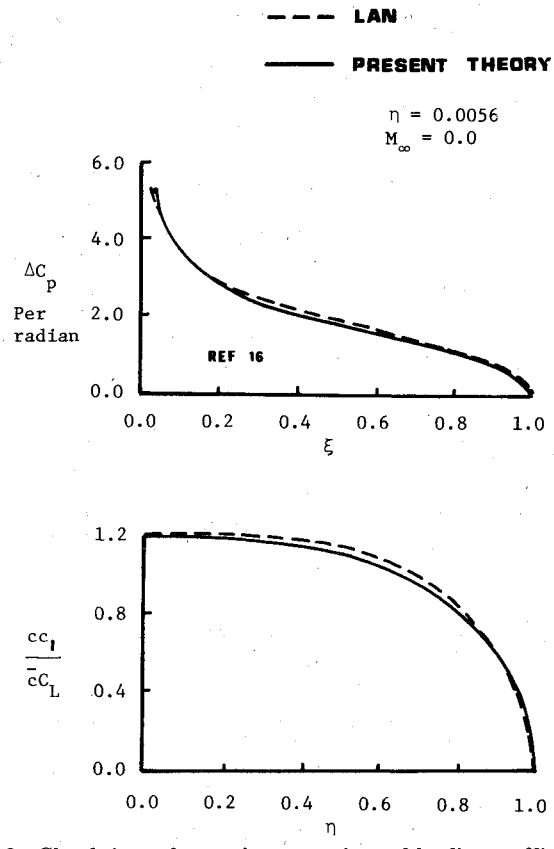

Fig. 9 Chordwise and spanwise comparison of loading coefficients with the method of Lan.

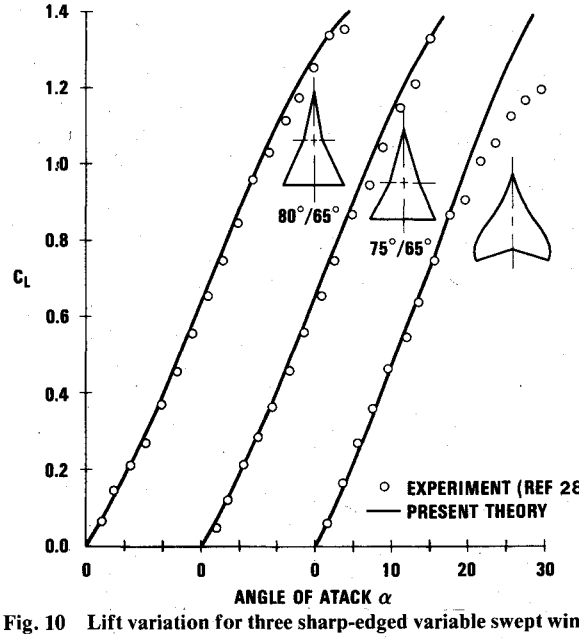

Fig. 10 Lift variation for three sharp-edged variable swept wings.

method is based on 3 chordwise and 4 spanwise control points with a 45 × 45-element mesh per panel.

Conclusions

In conclusion, the validity and accuracy of lifting-surface theory has been well established in the literature. The method proposed herein for solving the lifting-surface integral uses lifting line, thin airfoil, and slender wing theory results to develop a general functional form for the ΔC_p distribution. Evaluation of the Kernel function integral is accomplished in

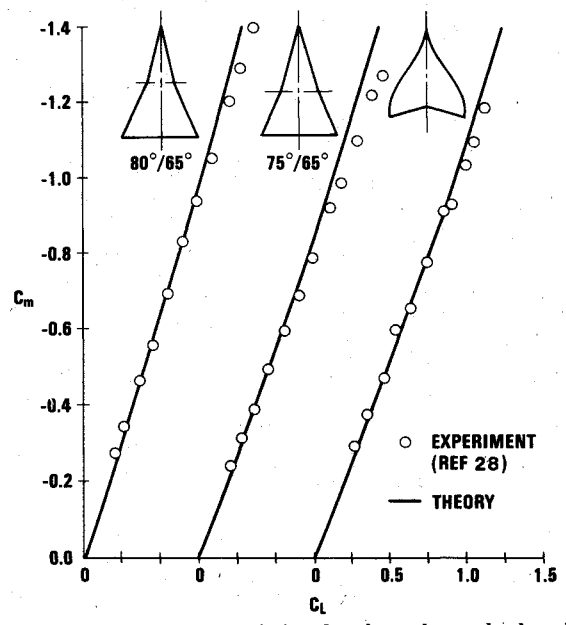

Fig. 11 Pitching moment variation for three sharp-edged variable swept wings.

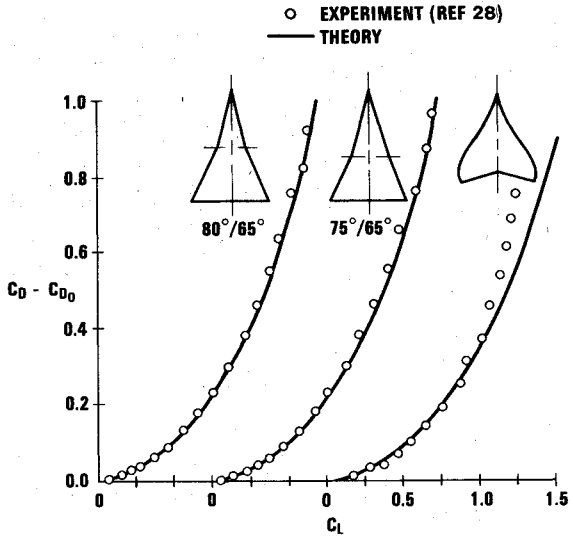

Fig. 12 Induced drag variation for three sharp-edged variable swept wings.

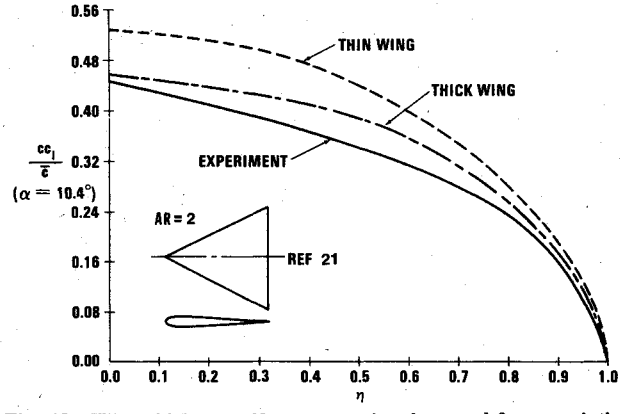

Fig. 13 Wing thickness effects on sectional normal force variations for a delta wing; $\mathcal{R} = 2$, $\alpha = 10.4$ deg.

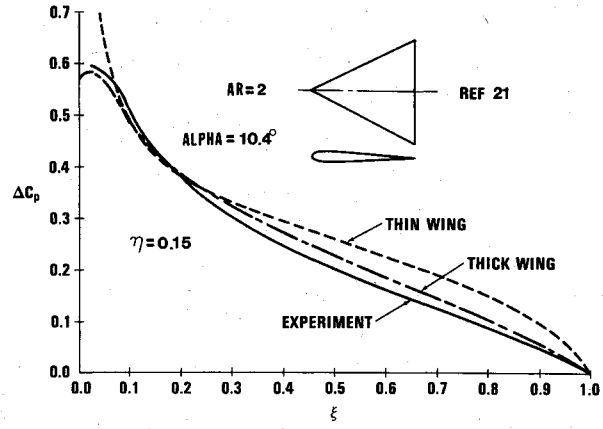

Fig. 14 Chordwise pressure variation for a thick delta wing; $\mathcal{R} = 2$, $\alpha = 10.4$ deg, $\eta = 0.15$.

a closed form/finite summation manner, rather than by numerical integration or a quadrature formula such as that of Gauss. The necessity of dealing with singularity and discontinuity problems in the Kernel is eliminated. Section lift, induced drag, and pitching moment, as well as total lift and induced drag, are given by closed-form summations. Total lift and induced drag results agree with the classical lifting line results.

The method retains the inherent advantages of lifting-surface theory, i.e., providing a continuous and realistic load distribution over the surface, satisfying the tangency condition over most of the wing, and requiring a solution for relatively few unknowns. In addition, the resulting mathematical form is easy to program and computationally fast. Wing load distributions compare extremely well with experiment, and if the airfoil section is sufficiently thin, accurate results are obtained at Mach numbers up to 0.85 even for low-$\mathcal{R}$ delta wings.

Convergence problems and oscillations in predicted pressure distributions, which are characteristic of distributed singularity techniques and are generally solved by using special pressure functions and/or least-squares formulations, have not appeared in any usage of the method to date. The coefficient matrix is well behaved, as with vortex lattice methods, and is solved quite adequately by Gaussian elimination rather than inversion or iteration.

References

[1] Smith, A. M. O. and Pierce, J., "Exact Solution of the Neumann Problem. Calculation of the Non-Circulatory Plane and Axially Symmetric Flow About or Within Arbitrary Boundaries," Douglas Aircraft Co., Rept. ES 26988, Aug. 1958.

[2] Bradley, R. G. and Miller, B. D., "Application of Finite Element Theory to Airplane Configurations," *Journal of Aircraft*, Vol. 8, June 1971, pp. 400-405.

[3] Woodward, F. A., "Analysis and Design of Wing-Body Combinations at Subsonic and Supersonic Speeds," *Journal of Aircraft*, Vol. 5, June 1968, pp. 528-534.

[4] *Vortex Lattice Utilization Workshop*, NASA SP-405, 1976.

[5] Landahl, M. T. and Stark, V. J. E., "Numerical Lifting Surface Theory—Problems and Progress," *AIAA Journal*, Vol. 6, Nov. 1968, pp. 2049-2060.

[6] Ashley, H. and Rodden, W. P., "Wing-Body Aerodynamic Interaction," *Annual Review of Fluid Mechanics*, Vol. 4, 1972, pp. 431-472.

[7] Chadwick, W., "The Application of Non-Planar Lifting Surface Theory to the Calculation of External Store Loads," U. S. Naval Weapons Laboratory, TR-2696, 1971.

[8] Cunningham, A. M., "Unsteady Subsonic Collocation Method for Wings With and Without Control Surfaces," *Journal of Aircraft*, Vol. 9, June 1972, pp. 413-419.

[9]Tulinius, J., "Theoretical Prediction of Wing-Fuselage Aerodynamic Characteristics at Subsonic Speeds," North American Rockwell Corp., Rept. NA-69-789.

[10]Bandler, P. A., "A Program to Calculate the Pressure Distribution on a Hydrofoil of Finite Span Near the Free Surface," Engineering Research Associates, Rept. 53/4, 1966.

[11]Lamar, J. E., "A Modified Multhopp Approach for Predicting Lifting Pressures and Camber Shape for Composite Planforms in Subsonic Flow," NASA TN D-4427, 1968.

[12]Wagner, S., "On the Singularity Method of Subsonic Lifting-Surface Theory," *Journal of Aircraft,* Vol. 6, Nov.-Dec. 1969, pp. 549-558.

[13]Ashley, H., Widnall, S., and Landahl, M., "New Directions in Lifting Surface Theory," *AIAA Journal,* Vol. 3, Jan. 1965, pp. 3-16.

[14]Rowe, W. S., Radman, M. C., Ehlers, F. E., and Sebastian, J. D., "Prediction of Unsteady Aerodynamic Loadings Caused by Leading Edge and Trailing Edge Control Surface Motions in Subsonic Compressible Flow—Analysis and Results," NASA CR-2543, Aug. 1975.

[15]Davies, D., "Generalized Aerodynamic Forces on a T-Tail Oscillating Harmonically in Subsonic Flow," British A.R.C, R&M 3422, 1964.

[16]Lan, C. E., "A Quasi-Vortex Lattice Method in Thin-Wing Theory," *Journal of Aircraft,* Vol. 11, Sept. 1974, pp. 516-527.

[17]DeJarnette, F. R., "Arrangement of Vortex Lattices on Subsonic Wings," *Vortex-Lattice Utilization Workshop,* NASA SP-405, 1976, pp. 301-323.

[18]Purvis, J. W., "Analytical Prediction of Vortex Lift," AIAA Paper 79-0363, 1979; see also *Journal of Aircraft,* Vol. 18, April 1981, pp. 225-230.

[19]Wang, H. T., "Comprehensive Evaluation of Six Thin-Wing Lifting-Surface Computer Programs," Naval Ship Research and Development Center, Rept. 4333, June 1974.

[20]Langan, T. J. and Wang, H. T., "Evaluation of Lifting-Surface Programs for Computing the Pressure Distribution on Planar Foils in Steady Motion," Naval Ship Research and Development Center, Rept. 4021, May 1973.

[21]Wick, B. H., "Chordwise and Spanwise Loadings Measured at Low Speed on a Triangular Wing Having an Aspect Ratio of Two and an NACA 0012 Airfoil Section," NACA TN 1650, June 1948.

[22]Rather, G. A., Hanson, C. M., and Rolls, L. S., "Investigation of a Thin Straight Wing of Aspect Ratio 4 by the NACA Wing-Flow Method, Lift and Pitching Moment Characteristics of the Wing Alone," NACA RM A8L20, 1948.

[23]Kolbe, C. D. and Tinling, B. E., "Tests of a Triangular Wing of Aspect Ratio 2 in the Ames Twelve-Foot Pressure Wind Tunnel," NACA RM A8E21, Sept. 1948.

[24]Margason, R. J. and Lamar, J. E., "Vortex-Lattice FORTRAN Program for Estimating Subsonic Aerodynamic Characteristics of Complex Planforms," NASA TN D-6142, 1971.

[25]Lopez, M. L. and Shen, C. C., "Recent Developments in Jet Flap Theory and Its Application to STOL Aerodynamic Analysis," AIAA Paper 71-578, 1971.

[26]Falkner, V. M. and Lehrian, D. E., "Low-Speed Measurements of the Pressure Distribution at the Surface of a Swept-Back Wing," British A.R.C., R&M 2741, 1953.

[27]Graham, R. R., "Low-Speed Characteristics of a 45° Swept-Back Wing of Aspect Ratio 8 from Pressure Distributions and Force Tests at Reynolds Numbers from 1,500,000 to 4,800,000," NACA RM L51.H13, 1951.

[28]Wentz, W. H. and Kohlman, D. L., "Wind Tunnel Investigation of Vortex Breakdown on Slender Sharp-Edged Wings," NASA CR-98737, Nov. 1968.